World J Surg (2016) 40:2976–2983
DOI 10.1007/s00268-016-3652-5

ORIGINAL SCIENTIFIC REPORT

Risk Factors for Predicting Occult Lymph Node Metastasis in Patients with Clinical Stage I Non-small Cell Lung Cancer Staged by Integrated Fluorodeoxyglucose Positron Emission Tomography/Computed Tomography

Kaoru Kaseda[1] · Keisuke Asakura[1] · Akio Kazama[2] · Yukihiko Ozawa[3]

Published online: 25 July 2016

Abstract

Background Lymph nodes in patients with non-small cell lung cancer (NSCLC) are often staged using integrated 18F-fluorodeoxyglucose positron emission tomography/computed tomography (FDG-PET/CT). However, this modality has limited ability to detect micrometastases. We aimed to define risk factors for occult lymph node metastasis in patients with clinical stage I NSCLC diagnosed by preoperative integrated FDG-PET/CT.

Methods We retrospectively reviewed the records of 246 patients diagnosed with clinical stage I NSCLC based on integrated FDG-PET/CT between April 2007 and May 2015. All patients were treated by complete surgical resection. The prevalence of occult lymph node metastasis in patients with clinical stage I NSCLC was analysed according to clinicopathological factors. Risk factors for occult lymph node metastasis were defined using univariate and multivariate analyses.

Results Occult lymph node metastasis was detected in 31 patients (12.6 %). Univariate analysis revealed CEA ($P = 0.04$), SUV_{max} of the primary tumour ($P = 0.031$), adenocarcinoma ($P = 0.023$), tumour size ($P = 0.002$) and pleural invasion ($P = 0.046$) as significant predictors of occult lymph node metastasis. Multivariate analysis selected SUV_{max} of the primary tumour ($P = 0.049$), adenocarcinoma ($P = 0.003$) and tumour size ($P = 0.019$) as independent predictors of occult lymph node metastasis.

Conclusions The SUV_{max} of the primary tumour, adenocarcinoma and tumour size were risk factors for occult lymph node metastasis in patients with NSCLC diagnosed as clinical stage I by preoperative integrated FDG-PET/CT. These findings would be helpful in selecting candidates for mediastinoscopy or endobronchial ultrasound-guided transbronchial needle aspiration.

Abbreviations

AUC	Area under the curve
CEA	Carcinoembryonic antigen
CT	Computed tomography
EBUS-TBNA	Endobronchial ultrasound-guided transbronchial needle aspiration
FDG-PET	18F-fluorodeoxyglucose positron emission tomography
NEMA	National Electrical Manufacturers' Association
NPV	Negative predictive value
NSCLC	Non-small cell lung cancer
ROC	Receiver operating characteristics
ROI	Region of interest
SABR	Stereotactic ablative radiotherapy

✉ Kaoru Kaseda
kaseda@wb4.so-net.ne.jp

[1] Department of Thoracic Surgery, Sagamihara Kyodo Hospital, 2-8-18 Hashimoto, Midori-ku, Sagamihara, Kanagawa 252-5188, Japan

[2] Department of Pathology, Sagamihara Kyodo Hospital, Kanagawa, Japan

[3] Yuai Clinic, Kanagawa, Japan

SUV_{max}	Maximum standardized uptake value
TNM	Tumour node metastasis
VOI	Volume of interest
WHO	World Health Organization

Introduction

Among all cancers, lung cancer remains the leading cause of death [1]. For patients with clinical stage I non-small cell lung cancer (NSCLC), the standard treatment is anatomical resection and systemic nodal dissection. However, about 25 % of patients are not amenable to lobectomy or pneumonectomy for various reasons. Limited surgery (wedge resection or segmentectomy) and new stereotactic ablative radiotherapy (SABR) are other options for such patients.

If clinical N0 tumours could be reliably identified, it would be possible to avoid anatomical resection and systemic nodal dissection. To achieve successful outcomes for SABR or limited surgery, it is necessary to perform accurate staging, especially of nodal metastasis. Being able to identify occult lymph node metastasis could improve outcomes and may permit individualized adjuvant systemic treatment beyond SABR or limited surgery. Important prognostic information can be obtained through accurate staging of NSCLC, and the best treatment approach can be determined.

Lymph nodes have been staged in patients with NSCLC using chest computed tomography (CT). Contrast-enhanced CT has become the most prevalent imaging modality for tumour node metastasis (TNM) staging, but it is limited in terms of evaluating lymph node status because positivity is predicted based only on node size [2]. Lymph nodes are being staged more frequently in patients with NSCLC using ^{18}F-fluorodeoxyglucose positron emission tomography (FDG-PET), which is based on the fact that glucose metabolism is typically increased in malignant cells [3]. New imaging systems using integrated FDG-PET/CT have recently been able to overcome the inherent disadvantages of FDG-PET, such as poor-quality anatomical information [4]. This integrated approach is more sensitive than CT alone in terms of lymph node staging for NSCLC [5]. As a practical approach, many centres schedule patients with negative mediastinal uptake on integrated FDG-PET/CT for resection [6].

The sensitivity and specificity of the ability of contrast-enhanced CT to predict mediastinal lymph node metastasis are 57–68 and 76–82 %, respectively [7, 8], whereas integrated FDG-PET/CT can identify nodal disease with 79–85 % sensitivity and 87–92 % specificity [7, 8]. Surgeons have widely applied integrated FDG-PET/CT to evaluate nodal metastasis. Currently, a practical approach adopted in many centres for SABR is to schedule patients with negative hilar and mediastinal lymph node uptake on integrated FDG-PET/CT for resection, preoperative mediastinoscopy or endobronchial ultrasound-guided transbronchial needle aspiration. The present study aimed to detect occult lymph node metastasis in patients with clinical stage I NSCLC diagnosed using preoperative integrated FDG-PET/CT. We also aimed to identify potential risk factors for nodal involvement, since it is expected that accurate prediction of occult lymph node involvement based on associated risk factors would facilitate the selection of appropriate candidates for preoperative mediastinoscopy or endobronchial ultrasound-guided transbronchial needle aspiration (EBUS-TBNA).

Patients and methods

Patient eligibility

A total of 444 consecutive patients underwent pulmonary resection for lung cancer at Sagamihara Kyodo Hospital (Sagamihara, Kanagawa, Japan) between April 2007 and May 2015. Among these, we reviewed the records of 246 who had clinical stage I NSCLC diagnosed by integrated FDG-PET/CT according to the 7th edition TNM classification and who underwent complete surgical resection by lobectomy or greater and systematic lymph node dissection. Complete resection was defined as the macroscopic and microscopic absence of residual cancer (R0). Patients were excluded if they underwent limited resection (segmentectomy or wedge resection), incomplete resection or neoadjuvant chemotherapy/radiotherapy. None of the patients underwent preoperative mediastinoscopy or EBUS-TBNA during this period.

We reviewed the following clinicopathological information: age, sex, smoking habit (never smoked or have smoked), history of lung disease, concurrent diabetes, preoperative serum carcinoembryonic antigen (CEA) level (cut-off at normal upper limit of 5.0 ng/mL), tumour laterality (right or left side), lobar distribution of tumour, tumour location, maximum standardized uptake value (SUV_{max}) of primary tumour, procedure, histological type, tumour size (cm), grade, pleural invasion (negative or positive) and lymph node metastasis (n0, n1 or n2). All clinical, intraoperative radiological and pathological findings were reviewed at two hospitals (Sagamihara Kyodo Hospital and Yuai Clinic, Kanagawa, Japan). The patient characteristics and preoperative tumour evaluations are shown in Table 1. Non-small cell lung carcinoma was diagnosed based on the World Health Organization (WHO) classification [9]. Pre- and postoperative TNM staging was applied [10]. The institutional review board at Sagamihara Kyodo Hospital approved the data collection and analyses

Table 1 Characteristics of patients and tumours ($n = 246$)

Variables	Distribution (%)
Age (years)	
Mean ± SD	69 ± 9.5
Range	35–86
Sex	
Female	146 (59.3)
Male	100 (40.7)
Smoking habits	
Non-smoker	96 (39.0)
Ever-smoker	150 (61.0)
History of lung disease[a]	
Absent	182 (74.0)
Present	64 (26.0)
Concurrent diabetes	
Absent	207 (84.1)
Present	39 (15.9)
CEA (ng/ml)	
≤5	187 (76.0)
>5	59 (24.0)
Tumour laterality	
Right	157 (63.8)
Left	89 (36.2)
Lobar distribution of tumour	
Right upper lobe	88 (35.8)
Right middle lobe	25 (10.2)
Right lower lobe	44 (17.9)
Left upper lobe	52 (21.1)
Left lower lobe	37 (15.0)
Tumour location	
Central	25 (10.2)
Non-central	221 (89.8)
SUV_{max} of tumour	
Median	3.0
Mean ± SD	4.4 ± 4.0
Range	0.5–28.3
Procedure	
Lobectomy	243 (98.4)
Bilobectomy	3 (1.2)
Pneumonectomy	1 (0.4)
Histological type	
Adenocarcinoma	191 (77.6)
Squamous cell carcinoma	39 (15.9)
Other types	16 (6.5)
Tumour size (cm)	
Median	2.8
Mean ± SD	3.1 ± 2.9
Range	0.5–18.0
Grade	
Well	162 (65.9)
Mod/poor	84 (34.1)
Pleural invasion (PL)	
Absent	217 (88.2)
Present	29 (11.8)
Lymph node metastasis	
n0	215 (87.4)
n1	13 (5.3)
n2	18 (7.3)

SUV_{max} maximum standardized uptake value, *CEA* carcinoembryonic antigen, *Well* well-differentiated carcinoma, *Mod/poor* moderately or poorly differentiated carcinoma

[a] History of lung disease includes interstitial lung disease, chronic obstructive pulmonary disorder, bronchial asthma and tuberculosis

and waived the need to obtain written informed consent from each patient during May 2015.

Computed tomography

All patients were assessed within four weeks of surgery using diagnostic-quality, contrast-enhanced CT of the chest with a slice thickness of 1 mm. A tumour was considered to be central if its centre was located in the inner one-third of the lung parenchyma (adjacent to the mediastinum) on transverse CT images. Tumours centred in the outer two-thirds of the lung parenchyma on transverse CT images were considered to be peripherally located tumours. The maximal diameter of lung nodules was measured on contrast-enhanced CT images of the chest.

Integrated ^{18}F-fluorodeoxyglucose positron emission tomography imaging

All patients were assessed by integrated FDG-PET/CT within four weeks before undergoing surgical resection. After fasting for six hours, FDG (3.5 MBq/kg body weight) was intravenously injected if the patient's blood sugar level was <200 mg/dL. Images were acquired from a single Eminence-SOPHIA PET/CT combined scanner (Shimadzu, Kyoto, Japan) starting 60 min later [11]. After attenuation correction, acquired image data were reconstructed using a dynamic row-action expectation maximization algorithm [12]. The reconstructed sectional images were then visually evaluated and quantified using the SUV_{max} inside a volume of interest (VOI) placed on lesions. The SUV_{max} was calculated as:

$$[(\text{maximum activity in VOI})/(\text{volume of VOI})]/[(\text{injected FDG dose})/(\text{patient weight})].$$

The quality of the radiation measurements was assured by calibration of the PET/CT scanner in accordance with the National Electrical Manufacturers Association (NEMA) NU-2 2001 standard [13].

Nodal uptake with $SUV_{max} > 2.5$ was considered positive [14–17]. A cylindrical region of interest (ROI) was manually placed over the transaxial site with the highest signal intensity to determine the SUV, which was normalized to the body weight of each patient. The SUV_{max} within a ROI served as our reference value [18].

Three experienced radiologists individually analysed integrated FDG-PET/CT images. If initial assessments differed, the final conclusion was reached by consensus.

Surgical resection

All patients underwent anatomical lung resection and radical lymphadenectomy conducted by thoracic surgeons at Sagamihara Kyodo Hospital. Nodal dissection techniques were standardized at the time of surgical resection. All systematic lymph node dissection proceeded according to the criteria of the American Thoracic Society, and at least three hilar and mediastinal stations each were removed.

Pathological examination

Experienced pulmonary pathologists assessed all resected tumour specimens, and NSCLC was histologically assessed based on the WHO classification. All dissected lymph nodes were stained with haematoxylin and eosin and then histologically assessed.

Statistical analysis

Data were statistically analysed using SPSS version 21.0 software (SPSS, Chicago, IL, USA). The optimal discriminative cut-off for SUV_{max} was assessed from receiver operating characteristic (ROC) curves. Predictors of lymph node metastasis in clinical stage I NSCLC using integrated FDG-PET/CT were identified by univariate analysis using Fisher's exact test or Pearson's Chi-square test. Independent predictors of occult lymph node metastasis of clinical stage I NSCLC were also assessed by multivariate analysis using logistic regression. Values of $P < 0.05$ were considered statistically significant.

Results

Patient characteristics

Table 1 shows the characteristics of the patient and pathological features of nodal involvement for 246 patients [female, $n = 146$; male, $n = 100$; mean age 69 (range 35–86) years]. The median tumour size was 2.8 cm, and the median SUV_{max} of the primary tumour was 3.0. One and three patients underwent total pneumonectomy and bilobectomy, respectively, and all others were treated by lobectomy.

Incidence of occult nodal metastasis

N1 and N2 disease involvement was evident in 13 (5.3 %) and in 18 (7.3 %) of the 246 patients, respectively. The negative predictive value (NPV) for occult lymph node metastasis on integrated FDG-PET/CT was 87.4 %.

Risk factors for occult lymph node metastasis

Figure 1 shows the ROC curve for predicting lymph node metastasis based on the SUV_{max} of the primary tumour, which had an area under the curve (AUC) of 0.665 ($P = 0.003$). The optimal cut-off for SUV_{max} of the primary tumour for occult lymph node metastasis determined from the ROC curve was 3.0. Table 2 shows predictors of lymph node metastasis in clinical stage I NSCLC selected by univariate analysis. The SUV_{max} of the primary tumour,

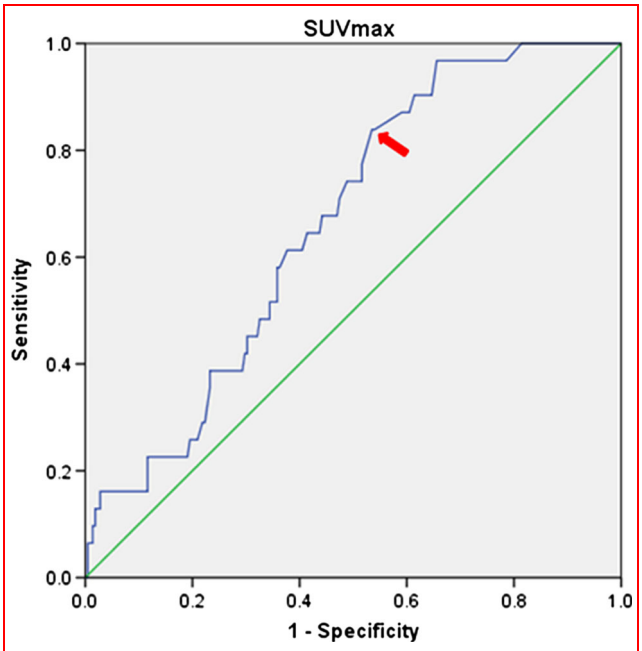

Fig. 1 Area under receiver operating characteristics curve for SUV_{max} of primary tumour to predict occult lymph node metastasis. AUC, 0.665 (95 % CI 0.578–0.751), $P = 0.003$. Hypothetical threshold SUV_{max} 3.0 (*arrow*) yielded 83.9 % sensitivity and 46.5 % specificity. AUC, area under the receiver operating characteristics curve; SUV_{max}, maximum standardized uptake value

Table 2 Univariate analysis of factors associated with occult lymph node metastasis

Variables	Pathological N0	Pathological N1–N2	*P* value
Age (years)			
≤65	8	9	N/S
>65	148	22	
Sex			
Female	129	17	N/S
Male	86	14	
Smoking habits			
Non-smoker	82	14	N/S
Ever-smoker	133	17	
History of lung disease			
Absent	158	24	N/S
Present	57	7	
Concurrent diabetes			
Absent	182	25	N/S
Present	33	6	
CEA (ng/ml)			
≤5	168	19	0.040*
>5	47	12	
Tumour laterality			
Right	136	21	N/S
Left	79	10	
Lobar distribution of tumour			
Upper or middle lobe[a]	146	19	N/S
Lower lobe[b]	69	12	
Tumour location			
Central	196	25	N/S
Non-central	19	6	
SUV_{max} of tumour			
≤3	114	10	0.031*
>3	101	21	
Histological type			
Adenocarcinoma	162	29	0.023*
Other types	53	2	
Tumour size (cm)			
≤3	132	10	0.002*
>3	83	21	
Grade			
Well	141	21	N/S
Mod/poor	74	10	
Pleural invasion (PL)			
Absent	193	24	0.046*
Present	22	7	

SUV_{max} maximum standardized uptake value, *CEA* carcinoembryonic antigen, *Well* well-differentiated carcinoma, *Mod/poor* moderately or poorly differentiated carcinoma

* Significance

[a] Upper or middle lobe includes right upper lobe, right middle lobe and left upper lobe

[b] Lower lobe includes right lower lobe, left lower lobe

histological type (adenocarcinoma) and tumour size represented independent predictors of occult lymph node metastasis for patients with clinical stage I NSCLC determined by integrated FDG-PET/CT according to multivariate analysis (Table 3). Table 4 shows predictors of mediastinal lymph node metastasis in clinical stage I NSCLC diagnosed by integrated FDG-PET/CT. The SUV_{max} of the primary tumour, histological type (adenocarcinoma) and tumour size were independent predictors of occult mediastinal lymph node metastasis of clinical stage I NSCLC by integrated FDG-PET/CT.

Follow-up

The median postoperative follow-up period was 4.5 years. Cancer recurred in 43 (17.5 %) of the 246 patients [intrathoracic recurrence, $n = 21$ (8.6 %); distant metastasis, $n = 22$ (8.9 %)]. Distribution of number of the patients with recurrence was as follows: N0 disease, $n = 18$ (7.3 %); N1 disease, $n = 10$ (4.1 %); N2 disease, $n = 15$ (6.1 %). And 30 (12.2 %) of the 246 patients had died of lung cancer by the end of the follow-up. Distribution of number of the patients with death was as follows: N0 disease, $n = 10$ (4.1 %); N1 disease, $n = 7$ (2.8 %); N2 disease, $n = 13$ (5.3 %).

Discussion

FDG-PET is widely used in the staging of NSCLC [14], and it should become a promising optimization tool for lymph nodal staging. Although integrated FDG-PET/CT provides useful information about hilar and mediastinal nodal metastases in lung cancer, microscopic lymph node metastases are barely detectable on integrated FDG-PET/CT.

We applied the traditional SUV_{max} cut-off of 2.5, and thus hilar and mediastinal lymph nodes with $SUV_{max} \geq 2.5$ were considered positive.

Occult lymph node metastasis was detected in 31 (12.6 %) of 246 patients, and the NPV was 87.4 %, which is in agreement with previous studies [19–24]. Not all patients underwent systematic lymph node dissection in some studies [19, 20], which might have resulted in underestimation of the true prevalence of occult nodal disease. In the present study, all patients underwent anatomical lung resection and radical lymphadenectomy. All systematic lymph node dissection proceeded according to the criteria of the American Thoracic Society, and at least three hilar and mediastinal stations each were removed. It seemed to be very important to perform anatomical lung resection and radical lymphadenectomy for accurate diagnosis of nodal status.

Table 3 Multivariate analysis of factors associated with occult lymph node metastasis

Variables	Odds ratio	95 % CI	*P* value
SUV_{max} of tumour (>3)	2.614	1.01–6.839	0.049*
Histological type (adenocarcinoma)	16.150	2.59–100.09	0.003*
Tumour size (>3 cm)	2.969	1.20–7.345	0.019*

SUV_{max} maximum standardized uptake value, *CI* confidence interval

* Significance

Table 4 Univariate and multivariate analysis of factors associated with occult mediastinal lymph node metastasis

Variables	Univariate analysis			Multivariate analysis		
	Odds ratio	95 % CI	*P* value	Odds ratio	95 % CI	*P* value
SUV_{max} of tumour (>3)	2.411	1.21–6.839	0.042*	2.218	1.34–6.541	0.049*
Histological type (adenocarcinoma)	14.150	1.88–99.29	0.008*	10.230	2.87–89.69	0.01*
Tumour size (>3 cm)	3.122	1.20–7.542	0.023*	2.645	1.38–6.923	0.031*

SUV_{max} maximum standardized uptake value, *CI* confidence interval

* Significance

The use of routine mediastinoscopy is not cost-effective for patients with peripheral stage I disease because the incidence of mediastinal disease among more central lesions is a known observation by many. And stage I NSCLC represents a heterogeneous group of tumours, so it is important to examine the risk factors for occult lymph node metastasis.

Univariate analysis significantly associated CEA, SUV_{max} of the primary tumour, adenocarcinoma, tumour size and pleural invasion with occult lymph node metastasis. Among patients with clinical stage I NSCLC determined by integrated FDG-PET/CT, multivariate analysis identified SUV_{max} of the primary tumour, adenocarcinoma and tumour size to be independent predictors of occult lymph node metastasis.

The incidence of lymph node metastasis increases as tumour size increases [25, 26]. Asamura et al. reported that the prevalence of lymph node metastasis increased from 19.5 % in tumours $\leq$2.0 cm in diameter to 32.5 % in tumours 2.0–3.0 cm in diameter in patients with resected peripheral NSCLC [26]. Large clinical tumours were significantly associated in the present study with an increased prevalence of occult lymph node metastases.

The clinical importance and relevance of SUV_{max} for primary NSCLC have been demonstrated. Several previous studies have reported that a higher SUV_{max} for primary NSCLC was significantly associated with nodal involvement, although the definition of the SUV threshold considerably varies among studies [4, 17, 23, 27, 28]. SUV_{max} provides information about biological aggressiveness, key pathological features and the potential for tumour spread. SUV_{max} of the primary tumour should be provided by radiologists in the text of every integrated FDG-PET/CT report.

Adenocarcinoma was also a risk factor for occult lymph node metastasis in our patients. Kanzaki et al. [29] considered that occult lymph node metastasis was more likely to occur in patients with lung adenocarcinoma. In contrast, Al-Sarraf et al. [6] reported that primary tumour cell type did not affect the incidence of occult MLN metastasis.

Lymph node metastases more frequently have a short-axis diameter $\leq$1 cm when they arise from adenocarcinoma than from squamous cell carcinoma [2]. Therefore, we speculate that patients with lymph node metastasis from squamous cell carcinoma might have been excluded from the series by Kanzaki et al., but would have been included in our series of patients.

From our results, we speculate that the SUV_{max} of the primary tumour, adenocarcinoma and tumour size reflect biological aggressiveness of the tumour. Integrated FDG-PET/CT will remain an important tool in the management of NSCLC, but is not a good stand-alone diagnostic tool and must be used with other patient characteristics in determining whether to refer a patient for tissue procurement.

The retrospective design is the main limitation of the present study. Prospective or randomized trials are warranted to clarify the true incidence of occult lymph node metastasis among patients with negative lymph node uptake on integrated FDG-PET/CT. We did not stage mediastinal invasion, which might have changed the denominator of truly occult disease. We excluded patients who had been treated by neoadjuvant chemotherapy and radiotherapy and those who underwent segmentectomy, to

avoid considerable inaccuracies. Although our criteria might have caused some degree of selection bias, the overall number of patients was probably large enough to overcome it.

The SUV_{max} of the primary tumour, adenocarcinoma and tumour size were risk factors for occult lymph node metastasis in patients with NSCLC diagnosed as clinical stage I by preoperative integrated FDG-PET/CT. False-negative results are inevitable, but may be somewhat predictable using some risk factors. These findings would be helpful in selecting patients who would benefit from preoperative mediastinoscopy or EBUS-TBNA. Our findings might facilitate pretherapy evaluation and decision-making.

Acknowledgments The author thanks Mr. Tomoyuki Kanno, Yuai Clinic, for data acquisition.

Compliance with ethical standards

Conflict of interest The authors have no conflicts of interest to disclose that would affect this article.

References

1. Jemal A, Siegel R, Ward E et al (2007) Cancer statistics, 2007. CA Cancer J Clin 57:43–66
2. Kamiyoshihara M, Kawashima O, Ishikawa S et al (2001) Mediastinal lymph node evaluation by computed tomographic scan in lung cancer. J Cardiovasc Surg (Torino) 42:119–124
3. Rohren EM, Turkington TG, Coleman RE (2004) Clinical applications of PET in oncology. Radiology 231:305–332
4. Cerfolio RJ, Ojha B, Bryant AS et al (2004) The accuracy of integrated PET-CT compared with dedicated PET alone for the staging of patients with nonsmall cell lung cancer. Ann Thorac Surg 78:1017–1023
5. Lardinois D, Weder W, Hany TF et al (2003) Staging of non-small-cell lung cancer with integrated positron-emission tomography and computed tomography. N Engl J Med 348:2500–2507
6. Al-Sarraf N, Aziz R, Gately K et al (2008) Pattern and predictors of occult mediastinal lymph node involvement in non-small cell lung cancer patients with negative mediastinal uptake on positron emission tomography. Eur J Cardiothorac Surg 33:104–109
7. Birim O, Kappetein AP, Stijnen T et al (2005) Meta-analysis of positron emission tomographic and computed tomographic imaging in detecting mediastinal lymph node metastases in nonsmall cell lung cancer. Ann Thorac Surg 79:375–382
8. Toloza EM, Harpole L, McCrory DC (2003) Noninvasive staging of non-small cell lung cancer: a review of the current evidence. Chest 123(1 Suppl.):137S–146S
9. World Health Organization (2004) Histological typing of lung and pleural tumours, 4th edn. IARC Press, Lyon
10. Goldstraw P, Crowley J, Chansky K, International Association for the Study of Lung Cancer International Staging Committee, Participating Institutions et al (2007) The IASLC Lung Cancer Staging Project: Proposals for the revision of the TNM stage groupings in the forthcoming (seventh) edition of the TNM classification of malignant tumours. J Thorac Oncol 2:706–714
11. Matsumoto K, Kitamura K, Mizuta T et al (2006) Performance characteristics of a new 3-dimensional continuous-emission and spiral-transmission high-sensitivity and high-resolution PET camera evaluated with the NEMA NU 2-2001 standard. J Nucl Med 47:83–90
12. Kitamura K, Ishikawa A, Mizuta T et al (2004) 3D continuous emission and spiral transmission scanning for high-throughput whole-body PET. In: Nuclear science symposium conference record 2004 IEEE, vol 5, pp 2801–2805
13. NEMA (2001) Performance measurements of positron emission tomographs. NEMA Standards Publication NU 2-2001. NEMA, Rosslyn
14. Fischer B, Lassen U, Mortensen J et al (2009) Preoperative staging of lung cancer with combined PET-CT. N Engl J Med 361:32–39
15. Okada M, Nakayama H, Okumura S et al (2011) Multicenter analysis of high-resolution computed tomography and positron emission tomography/computed tomography findings to choose therapeutic strategies for clinical IA lung adenocarcinoma. J Thorac Cardiovasc Surg 141:1384–1391
16. Hu M, Han A, Xing L et al (2011) Value of dual-time-point FDG PET/CT for mediastinal nodal staging in non-small-cell lung cancer patients with lung comorbidity. Clin Nucl Med 36:429–433
17. Iwano S, Ito S, Tsuchiya K et al (2013) What causes false-negative PET findings for solid-type lung cancer? Lung Cancer 79:132–136
18. Nabi HA, Zubeldia JM (2002) Clinical applications of F18-FDG in oncology. J Nucl Med Technol 30:3–9
19. Park HK, Jeon K, Koh WJ et al (2010) Occult nodal metastasis in patients with non-small cell lung cancer at clinical stage IA by PET/CT. Respirology 15:1179–1184
20. Veeramachaneni NK, Battafarano RJ, Meyers BF et al (2008) Risk factors for occult nodal metastasis in clinical T1N0 lung cancer: a negative impact on survival. Eur J Cardiothorac Surg 33:466–469
21. Wang J, Welch K, Wang L et al (2012) Negative predictive value of positron emission tomography and computed tomography for stage T1–2N0 non-small-cell lung cancer: a meta-analysis. Clin Lung Cancer 13:81–89
22. Gómez-Caro A, Garcia S, Reguart N et al (2010) Incidence of occult mediastinal node involvement in cN0non-small cell lung cancer patients after negative uptake of positron emission tomography/computed tomography scan. Eur J Cardiothorac Surg 37:1168–1174
23. Casiraghi M, Travaini LL, Maisonneuve P et al (2011) Lymph node involvement in T1 non-small cell lung cancer: could glucose uptake and maximal diameter be predictive criteria? Eur J Cardiothorac Surg 39:e38–e43
24. Li X, Zhang H, Xing L et al (2012) Mediastinal lymph nodes staging by 18F-FDG PET/CT for early stage non-small cell lung cancer: a multicenter study. Radiother Oncol 102:246–250
25. Shields TW (2009) Pathology of carcinoma of the lung. In: Shields TW, LoCicero J, Reed CE, Feins RH (eds) General thoracic surgery, vol II, 7th edn. Lippincott Williams & Wilkins, New York, pp 1311–1340
26. Asamura H, Nakayama H, Kondo H et al (1996) Lymph node involvement, recurrence, and prognosis in resected small, peripheral, non-small cell lung carcinomas. Are these carcinomas candidates for video-assisted lobectomy? J Thorac Cardiovasc Surg 111:1125–1134
27. Bryant AS, Cerfolio RJ, Klemm KM et al (2006) Maximum standard uptake value of mediastinal lymph nodes on integrated FDG-PET-CT predicts pathology in patients with non-small cell lung cancer. Ann Thorac Surg 82:413–422 **discussion 422–423**
28. Nambu A, Kato S, Sato Y et al (2009) Relationship between maximum standardized uptake value (SUV_{max}) of lung cancer

and lymph node metastasis on FDG-PET. Ann Nucl Med 23:269–275
29. Kanzaki R, Higashiyama M, Fujiwara A et al (2011) Occult mediastinal lymph node metastasis in NSCLC patients diagnosed as clinical N0-1 by preoperative integrated FDG-PET/CT and CT: Risk factors, pattern, and histopathological study. Lung Cancer 71:333–337